Determining Position and Orientation of 6R Robot using Image Processing

Amin Habibnejad Korayem
School of Mechanical Engineering,
Iran University of Science and Technology, Tehran, Iran
E-mail: a_habibnejad@mecheng.iust.ac.ir

Ensieh Niyavarani & Saeed Rafee Nekoo
School of Mechanical Engineering,
Iran University of Science and Technology, Tehran, Iran
E-mail: nc_n85@yahoo.com, rafee@iust.ac.ir

Moharam Habibnejad Korayem*
School of Mechanical Engineering,
Iran University of Science and Technology, Tehran, Iran
E-mail: hkorayem@iust.ac.ir
*Corresponding author

Abstract: Stereo vision is one of the best image processing software to identify the environment of robot and allow its simultaneous process for providing three-dimensional measurement in an acceptable rate. On the one hand, vision measurement has simple structure and on the other hand it is independent from active machine or robot. Appropriate software and efficient programming could improve the performance with same hardware (cameras). In this paper, stereo vision robot localization is used and the main code is developed in open source computer vision (Open CV) environment. The mathematical relationship between the three-dimensional reference coordinates and the local coordinates for entire system is presented. The vision system is an independent unit consists of two high definition (HD) cameras, set in a rotary base. The application of this measurement provides the position and orientation of 6R robot to verify its current measurement system. Stereo vision improved the speed of the image processing in comparison with image processing of MATLAB Toolbox that led to online monitoring of trajectory. Experimental tests of the proposed method express the capability of stereo vision in practical operations as a supervisory section.

1   INTRODUCTION

Open CV is an open source library for image processing and computer vision. The main advantages of Open CV are its high speed, being proper for real-time applications in areas such as human-computer interaction, object detection, segmentation and recognition, face detection, motion detection, and robotic applications. Open CV is written in C and C++ and runs under Linux, Windows and Mac. Open CV library is used as a specific data type and operating models in image processing domain.

A manipulator without a proper feedback of its motion is just a complicated mechanism [1]. There are numerous systems operating with open loop controller (i.e., see [2]); nonetheless, closed loop feedback makes them more precise and robust in terms model uncertainty [3], [4]. A potentiometer is a common device to measure angular position, suitable for articulated arms [5], although slight nonlinearity in them makes the encoder a better option [6]. Contactless magnetic encoder was used in [6], to improve the feedback system. As a result, feedback system is very important for controlling purposes and one of the best way for measuring feedback is image processing.

Tucker et al. used infrared light reflective surface to find the end-pose status [7]. Brown by using the laser beam reflected by optical sensors and the data processed by the controller determined the position and orientation of the object [8]. Using a combination of laser and camera, position of the robot, position of end-effector was estimated. Hantak and Lastra employed a laser to scan three-dimensional objects [9]. One of the most important issues in the processing is edge detection which is usually done through software.

In this present paper the image processing technique is used to obtain the position and orientation of end-effector as an alternative measurement for verification. Not mechanically connected to the robot, independency, low cost and high flexibility are the advantages of this method. In addition, this present paper is using cameras and Open CV software to generate information about description of the three-dimensional unknown object; specifically, determination of the position and the orientation of gripper. The implementation of such algorithms was used for calibration techniques (camera calibration), medical imagery, stereo vision, color, geometric shape analysis, motion analysis, three-dimensional reconstruction [10].

Motivations to use Open CV: the advance vision of research is providing not only open but also optimized code for basic vision infrastructure. The disseminate vision of knowledge is providing a common infrastructure that developer could build on, so that the code would be more readily readable and transferable. The advance vision-based commercial applications is making portable, performance optimized code available for free with a license that did not require commercial applications to be open or free themselves. Open CV functions cover areas such as image processing and analysis, structural analysis, object-oriented, object and scene recognition, camera calibration and three-dimensional structure.

2   CAMERA POSITIONS, HARDWARE OF VISION SYSTEM

Different scenarios are able to be considered for setting the cameras: 1) a single camera fixed or installed on the host; 2) parallel camera; 3) orthogonal camera; 4) The combination of precedent models. As in Fig. 1, we can see a model of a robot consisting of a camera, and a robot in which the camera can be fixed or installed on the host. There is a difference between the way that only the object can be seen and the way that the object and gripper could be monitored. The first mode of the system is end-point open loop (EOL) and the latter method is end-point close loop (ECL). So the camera or the object will move in the direction perpendicular to the optical axis of the camera if the object is in the camera's workspace.

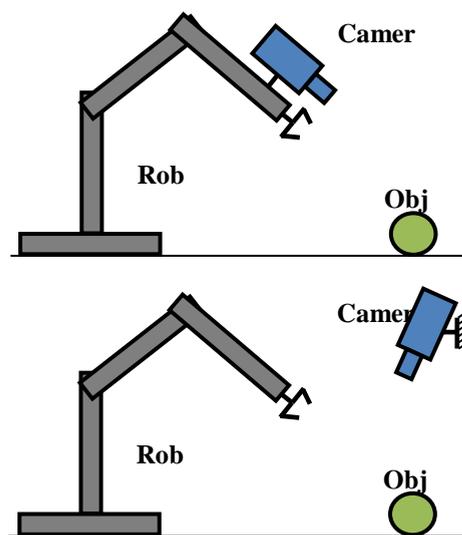**Fig. 1**   Using a camera to measure the position of the end-effector

The main difference between these two modes is that EOL system must be calibrated in hand-eye approach. It should be noted that just being in a position directly depends on the reliability of the calibration of hand-eye. In contrast to system observing the end-effector and object, its accuracy is independent of its hand-eye

calibration error. The first method simply put the only object in the camera's viewing area, but in ECL method the object and the gripper are seen by the camera. Therefore ECL is preferable to EOL. ECL system must feel the end-effector like an object, implementation of ECL controller needs to solve related problem to vision [11].

In this geometric model, two cameras are used. As it is shown in Fig. 2, the camera used in this research, is Microsoft Life Cam HD-6000, which has a good resolution, wide viewing angle, high-quality image and no zoom lens glasses. Zoom camera lens causes changes in calibration and may affect the calculations. Low quality of the images and the improper resolution will cause large error in calibration. In this work, the feasibility study and implementation of stereo vision are discussed as a three dimensional scanner for detecting object in stereo vision, using two cameras at a suitable distance from each other and looking at a scene.
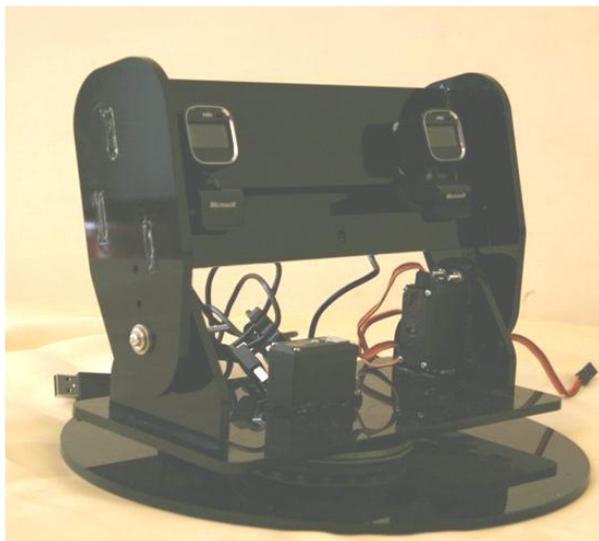

Fig. 2 The system of a two camera-HD 6000

Table 1 The Camera specifications [12]

Pixel size	3 μm X 3 μm
Image area	3888 μm X 2430 μm
Lens size	1/4"
S/N ratio	39 Db

The images are created in which the objects are registered with a view. If the object is closer to the stereo, the more parallax images will be recorded and vice versa. In this paper a feature is used to obtain the distance of each point of the image and therefore, it will result in three-dimensional information about the scene. According to the high credit of Microsoft, in

comparison to other manufacturers, the information of the camera's image sensor and internal data are available. The camera information is presented in Table 1. Signal to noise ratio is important to obtain good-quality data for image. The relatively large aperture lenses cause the image quality of the light. Having the pixel dimensions, the distance calculations are the resolution that can be done more easily and also the features of the camera will be extracted.

3   FORMULATIONS

In this section the mathematical relationship between the three-dimensional reference coordinates and the local coordinates in cameras is presented. As noted in this paper, two cameras are used. The geometric model is an object model and the two cameras have optical parallel axis. In optic, the triangular model is a very important principal for measuring in three-dimensional coordinates. In the triangular model, the object is seen from two different angles and the spatial position of the object is determined. The three-dimensional position of the points in space would make a triangle, Fig. 3.
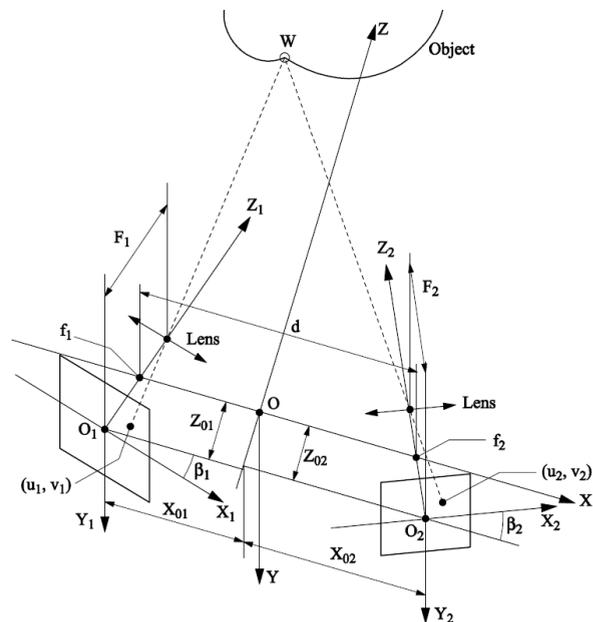
Fig. 3 Layout of the cameras and reference and local coordinates [13]

Reference coordinate system is marked with x, y, z, axes and its center is marked with o, x axis of the coordinate system, matches online, f_1, f_2 and axis Z is perpendicular to the line f_1, f_2. Point O is located at an equal distance to the line f_1, f_2. Two-dimensional coordinate system is located by the centers o_1 and o_2 and its coordinate axes are $x_1 y_1$ and $x_2 y_2$. The points f_1

and f_2 are the axis of rotation of each two cameras. The optical axis is perpendicular to the screen, were the cameras and z_1 and z_2 are in the local coordinate axes. A relationship can be found between the three-dimensional coordinates in the local and reference coordinate in cameras. This relationship is expressed by the matrix [13]:

$$M^T = RTP^T, \tag{1}$$

Where P and M are local and global positions of the object and have following forms:

$$P = [x, y, z, l], \tag{2}$$

$$M = [X, Y, Z, l]. \tag{3}$$

Also R and T matrices in Eq. (1) are rotation and translation matrices, respectively and have following shapes:

$$R = \begin{bmatrix} \cos\beta & 0 & \sin\beta & 0 \\ 0 & 1 & 0 & 0 \\ \sin\beta & 0 & \cos\beta & 0 \\ 0 & 0 & 0 & 1 \end{bmatrix}, \tag{4}$$

$$T = \begin{bmatrix} 1 & 0 & 0 & X_0 \\ 0 & 1 & 0 & Y_0 \\ 0 & 0 & 1 & Z_0 \\ 0 & 0 & 0 & 1 \end{bmatrix}, \tag{5}$$

Where in Eq. (4) β is the rotation of optical axis of considered camera and $[X_0, Y_0, Z_0]$ is position of center of local frame with respect to reference frame. Consider F as focal length, and then perspective relations for any image can be written as:

$$\frac{x}{u} = -\frac{z-F}{F}; \qquad \frac{y}{v} = -\frac{z-F}{F}. \tag{6}$$

Substituting Eq. (6) in Eq. (1), for two images, 3D position of the object in reference frame can be computed as:

$$X = \frac{u_1 F_1 - m_1 X_{01} - n_1(Z + Z_{01})}{m_1},$$

$$Y = v_1 - Y_{01} - \frac{v_1}{F_1}[(X - X_{01})\sin\beta_1$$
$$+ (Z - Z_{01})\cos\beta_1],$$

$$Z = [m_1 m_2 (X - X_{01}) + m_1 F_2 u_2 - m_2 F_1 u_1$$
$$+ m_2 n_1 Z_{01} - m_1 n_2 Z_{02}] / [m_1 n_2 - m_2 n_1] \tag{7}$$

New parameters in Eq. (7) are as follows:

$$m_1 = F_1 \cos\beta_1 + u_1 \sin\beta_1,$$
$$m_1 = F_2 \cos\beta_2 - u_2 \sin\beta_2,$$
$$n_1 = u_1 \cos\beta_1 - F_1 \sin\beta_1,$$
$$n_2 = u_2 \cos\beta_2 - F_2 \sin\beta_2, \tag{8}$$

Where $[u_i, v_i]$ is coordinate of the object project into i-th image. If two cameras are parallel with $\beta=0$ then following simple relations can be reached:

$$Y_{01} = Y_{02} = 0,$$
$$\beta_1 = \beta_2 = 0,$$
$$F_1 = F_2 = F, \tag{9}$$
$$X_{01} = X_{02} = \frac{B}{2}.$$

Finally Eq. (7) can be rewritten as:

$$X = \frac{F-Z}{F} u_1 - \frac{B}{2},$$
$$Y = \frac{F-Z}{F} v_1, \tag{10}$$
$$Z = F - \frac{BF}{u_1 - u_2},$$

Fig. 4 6R manipulator [5]

In which u_1-u_2 in Eq. (10) is the difference between the x coordinate of two corresponding pixels, named disparity. The disparity of an object that is in infinity is equal to zero.

4 6R ROBOT

The proposed vision system in Section 3 is implemented on 6R robot as a supervisory unit. The 6R manipulator is presented in Fig. 4 and the schematic of that is shown in Fig. 5. The Denavit-Hartenberg parameters of the arm are expressed in Table 2 and the specifications of the motors are presented in Table 3.
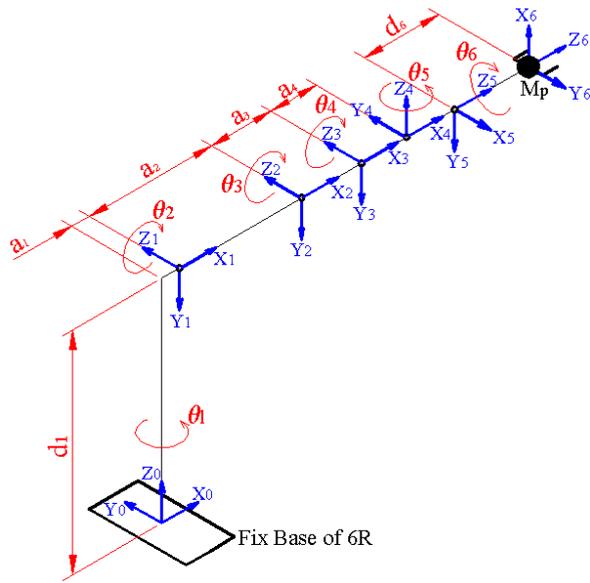

Fig. 5 Schematic of the arm [5]

Table 2 The Denavit-Hartenberg parameters

No.	a_i	d_i	$\alpha_i(°)$	θ_i
1	a_1=36.5 mm	d_1=438mm	-90	θ_1
2	a_2=251.5mm	0	0	θ_2
3	a_3=125 mm	0	0	θ_3
4	a_4=92 mm	0	90	θ_4
5	0	0	-90	θ_5
6	0	d_6=152.8mm	0	θ_6

Table 3 The specifications of the motors

Motor	1	2	3	4	5	6
U_{stall} (N.m)	114	98	382.2	40.4	40.4	40.4
ω_{stall} (rad/s)	1.3	1.04	0.73	0.9	0.9	0.9
Gear box ratio	1:333.2	1:10	1:500	1:50	1:50	1:50
Voltage (v)	12	24	12	12	12	12

The details of 6R robot: forward and inverse kinematics, Jacobian matrix and state-space representations of the system are presented in the following. The transformation matrix, T_0^6, is used for forward kinematics computations:

$$T_0^6 = \begin{bmatrix} n_x & o_x & a_x & p_x \\ n_y & o_y & a_y & p_y \\ n_z & o_z & a_z & p_z \\ 0 & 0 & 0 & 1 \end{bmatrix},$$

Where the elements of T_0^6 are as follows:

$n_x = -c_6 s_1 s_5 + c_1(c_{234} c_5 c_6 - s_{234} s_6),$

$n_y = c_{234} c_5 c_6 s_1 + c_1 c_6 s_5 - s_1 s_{234} s_6,$ $n_z = -c_5 c_6 s_{234} - c_{234} s_6,$

$o_x = s_1 s_5 s_6 - c_1(c_6 s_{234} + c_{234} c_5 s_6),$

$o_y = -c_6 s_1 s_{234} - (c_{234} c_5 s_1 + c_1 s_5) s_6,$ $o_z = -c_{234} c_6 + c_5 s_{234} s_6,$

$a_x = -c_5 s_1 - c_1 c_{234} s_5,$ $a_x = -c_5 s_1 - c_1 c_{234} s_5,$

$a_y = c_1 c_5 + c_{234} s_1 s_5,$ $a_z = s_{234} s_5,$

$p_x = -d_6 c_5 s_1 + c_1(a_1 + a_2 c_2 + a_3 c_{23} + c_{234}(a_4 - d_6 s_5)),$

$p_y = d_6 c_1 c_5 + s_1(a_1 + a_2 c_2 + a_3 c_{23} + c_{234}(a_4 - d_6 s_5)),$

$p_z = d_1 - a_2 s_2 - a_3 s_{23} + s_{234}(-a_4 + d_6 s_5).$

In these equations, a_i and d_i are shown in Fig. 5. Also s_i, c_i, s_{ij} and c_{ij} denote $\sin(\theta_i)$, $\cos(\theta_i)$, $\sin(\theta_i + \theta_j)$ and $\cos(\theta_i + \theta_j)$, respectively. The elements of the transformation matrix are used for obtaining the dynamics equation of 6R and end-effector position of the arm. The inverse kinematics equations of the manipulator were also needed for computing the initial conditions for links in simulations and experiments. The inverse kinematics equations are provided in the following:

$$\theta_1 = \tan^{-1}\left[\frac{p_y - d_6 a_y}{p_x - d_6 a_x}\right],$$

$$\theta_5 = \tan^{-1}\left[\frac{\pm d_6 \left[1 - (a_y C_1 - a_x S_1)^2\right]^{\frac{1}{2}}}{p_y C_1 - p_x S_1}\right],$$

$$\theta_2 + \theta_3 + \theta_4 = \theta_{234} = \tan^{-1}\left(\frac{-a_z}{a_x C_1 + a_y S_1}\right) \text{ for } \theta_5 > 0,$$

$\theta'_{234} = \theta_{234} + \pi \text{ for } \theta_5 < 0,$

$$\theta_6 = \tan^{-1}\left[\frac{o_x S_1 - o_y C_1}{n_y C_1 - n_x S_1}\right] \text{ for } \theta_5 > 0,$$

$\theta'_6 = \theta_6 + \pi \text{ for } \theta_5 < 0,$

$t = C_1 p_x + S_1 p_y + d_6 S_5 C_{234} - a_4 C_{234},$

$u = -p_z + d_1 - a_4 S_{234} + d_6 S_5 S_{234},$

$$w = \frac{-a_3^2 + t^2 + u^2 + a^{22}}{2a_2},$$

$$q = (t^2 + u^2)^{1/2},$$

$$\theta_2 = \tan^{-1}\left[\frac{\pm\left[1-(\frac{w}{q})^2\right]^{\frac{1}{2}}}{\frac{w}{q}}\right] + \tan^{-1}\left[\frac{u}{t}\right],$$

$$\theta_3 = \tan^{-1}\left[\frac{u-a_2 S_2}{t-a_2 C_2}\right] - \theta_2,\ \theta_4 = \theta_{234} - \theta_2 - \theta_3.$$

In inverse kinematics equations, the first angle and fifth one are computed at first. After that the summation of the angles of second, third and fourth links are obtained. Then the angle of the sixth links is calculated. There are two other configurations for summation of the angles of second, third and fourth links and sixth one. Introducing variables t, u, w and q, the angles of the second, third and fourth links are attained separately. The relation between the velocity of an end-effector and the angular velocity of joints, which is known as Jacobian matrix is expressed by $\dot{X} = J(q)\dot{q}$, where $q = \begin{bmatrix} \theta_1 & \theta_2 & ... & \theta_6 \end{bmatrix}^T$ is the angles of the links, $\dot{X} = \begin{bmatrix} \dot{p}_x & \dot{p}_y & \dot{p}_z \end{bmatrix}^T$ is the velocity vector of the end-effector of the manipulator, $J(q)$ is the Jacobian matrix and $\dot{q} = dq/dt$. The details of the Jacobian matrix is presented as:

$$J(q) = \begin{bmatrix} j_{11} & j_{12} & j_{13} & j_{14} & j_{15} & 0 \\ j_{21} & j_{22} & j_{23} & j_{24} & j_{25} & 0 \\ 0 & j_{32} & j_{33} & j_{34} & d_6 c_5 s_{234} & 0 \\ 0 & -s_1 & -s_1 & -s_1 & c_1 s_{234} & j_{46} \\ 0 & c_1 & c_1 & c_1 & s_1 s_{234} & j_{56} \\ 1 & 0 & 0 & 0 & c_{234} & s_{234} s_5 \end{bmatrix},$$

Where

$$j_{11} = -d_6 c_1 c_5 - s_1(a_1 + a_2 c_2 + a_3 c_{23} + c_{234}(a_4 - d_6 s_5)),$$

$$j_{12} = -c_1(a_2 s_2 + a_3 s_{23} + s_{234}(a_4 - d_6 s_2)),$$

$$j_{13} = -c_1(a_3 s_{23} + s_{234}(a_4 - d_6 s_5)),$$

$$j_{14} = c_1 s_{234}(-a_4 + d_6 s_5),$$

$$j_{15} = -d_6 c_1 c_{234} c_5 + d_6 s_1 s_5,$$

$$j_{21} = -d_6 s_1 c_5 + c_1(a_1 + a_2 c_2 + a_3 c_{23} + c_{234}(a_4 - d_6 s_5)),$$

$$j_{22} = -s_1(a_2 s_2 + a_3 s_{23} + s_{234}(a_4 - d_6 s_5)),$$

$$j_{23} = -s_1(a_3 s_{23} + s_{234}(a_4 - d_6 s_5)),$$

$$j_{24} = s_1 s_{234}(-a_4 + d_6 s_5),$$

$$j_{25} = -d_6(c_{234} c_5 s_1 + c_1 s_5),$$

$$j_{32} = -a_2 c_2 - a_3 c_{23} + c_{234}(-a_4 + d_6 s_5),$$

$$j_{33} = -a_3 c_{23} + c_{234}(-a_4 + d_6 s_5),$$

$$j_{34} = c_{234}(-a_4 + d_6 s_5),$$

$$j_{46} = -c_5 s_1 - c_1 c_{234} s_5,\ j_{56} = c_1 c_5 - c_{234} s_1 s_5.$$

Using the kinematics of the robot, the data of trajectory of the end-effector from vision system can be transferred into joint space for checking the error of robot in terms of joints.

5   EXPERIMENTAL TEST RESULTS

The camera base was vertically placed on a table, and also LEDs were placed vertically or horizontally on a separate base. It is preferred that LED position has the same height of the left camera and also it is in line with its optical axis. The point (0,0) has been in the center at the position with (638×350) pixel. Cameras were placed at a distance of 50cm from the arm. This experiment was repeated several times for reliability. By this measurement, three-dimensional position of LED was obtained and stored in the computer. With the aim of an HD camera and LED, several tests were done and the results were displayed using MATLAB software. Method of this test requires putting LED on the robot arm, and the robot arm started rotating till 90 degrees.
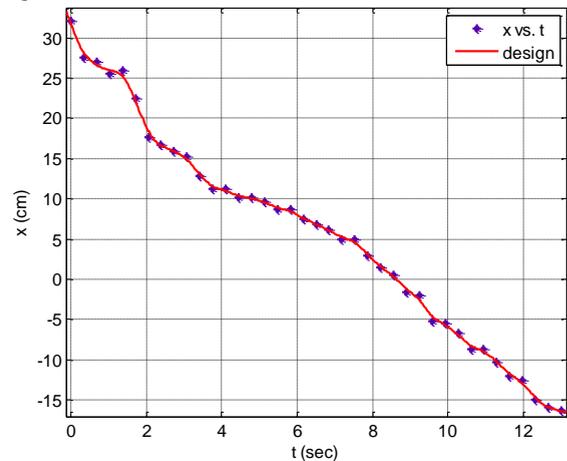

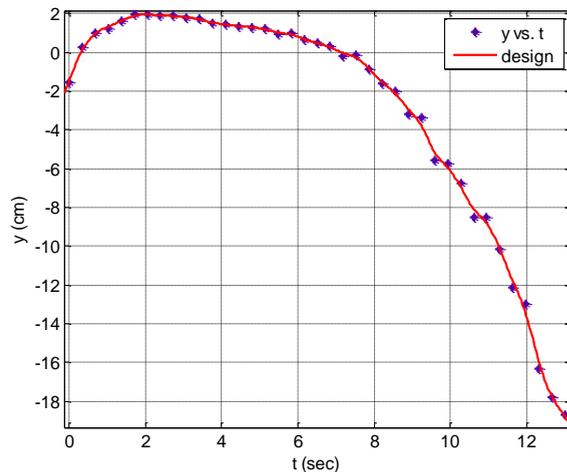**Fig. 6**   Variation of the end-effector in *x* axis
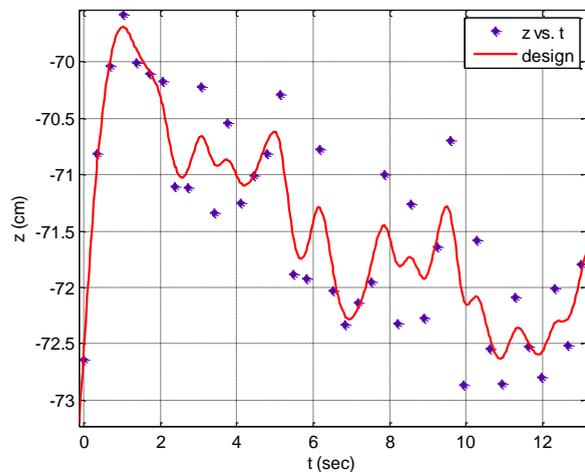

Fig. 7   Variation of the end-effector in *y* axis

Fig. 8 Variation of the end-effector in *z* axis

Fig. 9 Variation of the end-effector angle around *x* axis

And while the camera started taking pictures, the results was stored in a computer in the coordinate *X*, *Y*, *Z* and the given angle was computed by open CV.
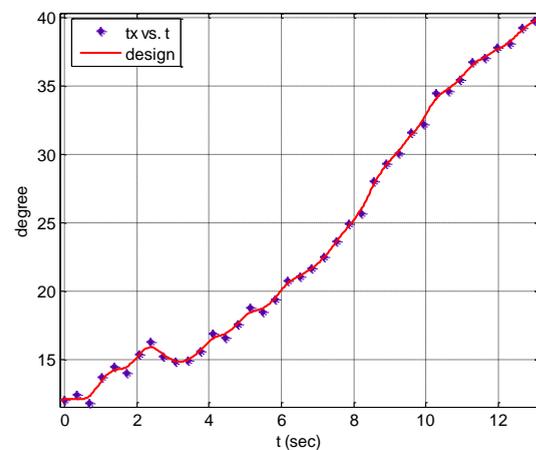
The variations of the end-effector in Cartesian coordinate are presented in Figs. 6-8 and the orientation of it in Figs. 9, 11-12. Moreover, the trajectory of the arm is illustrated in Fig. 10.
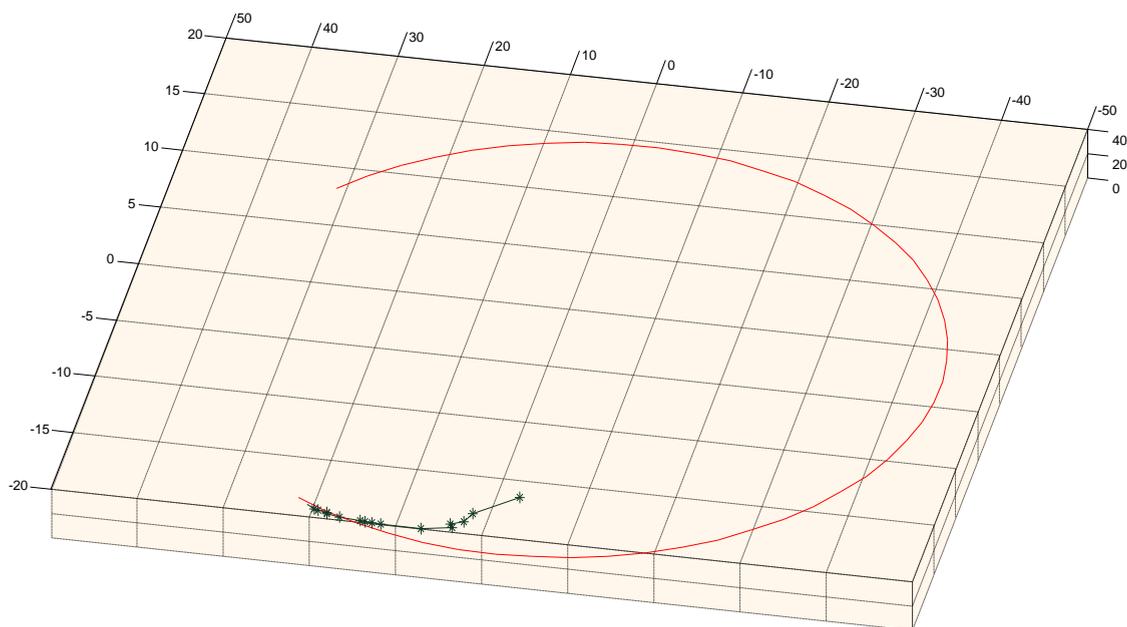

Fig. 10 End-effector trajectory in circular motion

Forty samples was considered for data recording, blue dots are the data taken by the cameras of the robot motion and the red line is drawn by MATLAB software as the desired trajectory. The robot arm tracked a little more than a quarter-circle. The horizontal axis is a time line chart. A camera captured images, 3 shots in a second. The Camera height to the robot arm was 65cm.

Open CV structure of the setup: The related functions of Open CV that allows us to implement the

image processing could be found in HighGUI library. With the aim of this library, we could create windows, read, write and etc. in the interface. HighGUI has three parts: hardware, operating system and GUI. The hardware works with the cameras, operating system plays the role of loading, saving and processing of the images, and the GUI section provides an interface for commanding.

Calibration of the cameras was benefited from "cvCalibrateCamera2()" command that helps users for

systematic calibration. The main key to calibration was putting a detectable object with clear edges as a sample for camera to analyze in different positions; checkerboard was a very useful object for this specific action in our tests. The sampling image processing time was 20ms and the tests were repeated 40 times for checking reliability. The sampling time was fixed 20ms after try and error for finding the suitable value. Bigger values reduced the precision and the ones less than 20ms increased the time of computations.
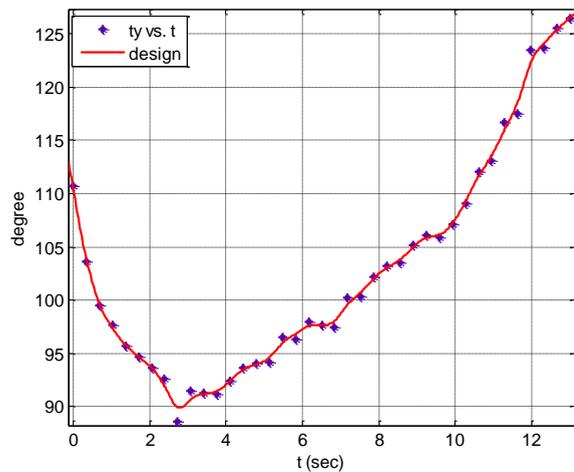

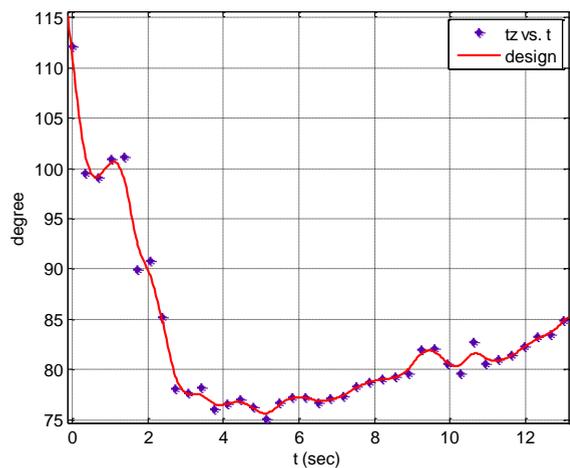**Fig. 11**   Variation of the end-effector angle around *y* axis

Fig. 12   Variation of the end-effector angle around *z* axis

6   CONCLUSION

Stereo vision method is selected, because of its advantages such as the low price, no mechanical connection to the end-effector and the high flexibility to identify the distance between the object and the robot. Considering that the sensors have a crucial role in flexibility of the system, in this paper, camera is used

as a sensor to acquire and process the information to obtain position of robot's end-effector. In order to reduce the errors, the robot and cameras must be carefully calibrated. The speed of the robot during motion and light of LED during capturing images must be set properly. In order to have better measurement, the following points should be regarded:

1) increasing the distance between two LEDs, so it will result in better outputs

2) environment's light should be such that it does not interfere with the LED's light

REFERENCES

[1]   Korayem, M. H., Nekoo, S. R., and Korayem, A. H., "Engineering Design of the Guidance System of the 6R Tele-robot based on DTMF", International Journal of Advanced Design and Manufacturing Technology, Vol. 7, No. 3, 15 Nov. 2014, pp. 57–63.

[2]   Karami, N., Korayem, M. H., Shafei, A. M., and Nekoo, S. R., "Theoretical and Experimental Investigation of Dynamic Load Carrying Capacity of Flexible-Link Manipulator in Point-to-Point Motion", Modares Mechanical Engineering, Vol. 14, No. 15, 2015, pp. 199-206. (In Persian)

[3]   Korayem, M. H., Irani, M., and Nekoo, S. R., "Analysis of Manipulators using SDRE: A Closed Loop Nonlinear Optimal Control Approach", Journal of Sciatica Iranica, Transaction B: Mechanical Engineering, Vol. 17, No. 6, 2010, pp. 456–467.

[4]   Korayem, M. H., Irani, M., and Nekoo, S. R., "Motion Control and Dynamic Load Carrying Capacity of Mobile Robot via Nonlinear Optimal Feedback", AMAE International Journal on Manufacturing and Material Science, Vol. 2, No. 1, 2012, pp. 16–21.

[5]   Korayem, M. H., Nekoo, S. R., and Abdollahi, F., "Hardware Implementation of a Closed Loop Controller on 6R Robot using ARM Microcontroller", International Research Journal of Applied and Basic Sciences, Vol. 4, No. 8, 2013, pp. 2147–2158.

[6]   Korayem, M. H., Nekoo, S. R., "State-Dependent Differential Riccati Equation to Track Control of Time-Varying Systems with State and Control Nonlinearities", ISA Transactions, Vol. 57, 2015, pp. 117–135.

[7]   Tucker, M., Perreira, M., and Nyman, D., "A Pose Measurement Sensor", Proc of the Workshop on Robot Standards, Detroit, Michigan, June 1985, pp. 2.83-2.98.

[8]   Brown, L. B., "A Random-Path Laser Interferometer System", In Proceedings of International Congress on Applications of Lasers and Electro-Optics, Nov. 1985.

[9]   Hantak, C., and Anselmo, L., "Metrics and Optimization Techniques for Registration of Color to Laser Range Scans", In Third International Symposium on 3D Data Processing, Visualization, and Transmission, Jun. 2006, pp. 551-558.

[10] Bradski, G., Kaehler, A., "Learning Open CV: Computer Vision with the Open CV Library", O'Reilly Media, Inc., 2008.

[11] Flandin, G., Chaumette, F., and Marchand, E., "Eye-in-Hand/Eye-to-Hand Cooperation for Visual Servoing", In Proceedings of IEEE International Conference on Robotics and Automation, Vol. 3, 2000, pp. 2741-2746.

[12] www.ovt.com

[13] Korayem, M. H., Irani, M., and Nekoo, S. R., "Application of Stereo Vision and ARM Processor for Motion Control", Interdisciplinary Mechatronics, 2013, pp. 483–499.